

1 **Long-term effects of the transient COD concentration on**  
2 **the performance of microbial fuel cells**

3  
4 **S. Mateo<sup>a</sup>, A. Gonzalez del Campo<sup>a</sup>, J. Lobato<sup>b</sup>, M. Rodrigo<sup>b</sup>, P. Cañizares<sup>b</sup>, F.J.**  
5 **Fernandez-Morales<sup>a\*</sup>**

6 <sup>a</sup> University of Castilla-La Mancha, Chemical Engineering Department, ITQUIMA, Avenida  
7 Camilo José Cela S/N. 13071 Ciudad Real, Spain.

8 <sup>b</sup> University of Castilla-La Mancha, Chemical Engineering Department, Faculty of Chemical  
9 Sciences & Technologies, Edificio Enrique Costa Novella, Avenida Camilo José Cela S/N.  
10 13071 Ciudad Real, Spain.

11  
12  
13  
14  
15 \* Corresponding author: Francisco Jesus Fernandez Morales

16 University of Castilla-La Mancha, ITQUIMA, Chemical Engineering Dept., Avda. Camilo  
17 José Cela S/N 13071, Ciudad Real, Spain.

18 Tel: 0034 926 295300 (ext. 6350), Fax: 0034 926 295242

19 E-mail: [FcoJesus.FMorales@uclm.es](mailto:FcoJesus.FMorales@uclm.es)

25 **Abstract**

26 In this work, the long-term effects of transient Chemical Oxygen Demands (COD)  
27 concentrations over the performance of a microbial fuel cell were studied. From the obtained  
28 results, it was observed that the repetitive change in the COD loading rate during 12 hours  
29 conditioned the behavior of the system during periods of up to 7 days. The main  
30 modifications were the enhancement of the COD consumption rate and the exerted current.  
31 These enhancements yielded increasing Coulombic Efficiencies (CEs) when working with  
32 COD concentrations of 300 mg/L, but constant CEs when working with COD concentrations  
33 from 900 to 1800 mg/L. This effect could be explained by the higher affinity for the substrate  
34 of *Geobacter* than that of the non-electrogenic organisms such as *Clostridia*.

35

36 **Keywords:** Microbial Fuel Cell; COD; long-term; electricity.

37

38

## 39 1. Introduction

40

41 The world population has experienced continuous growth during the last centuries. Current  
42 projections show a continuous increase of population up to approximately 9 billion  
43 inhabitants by the year 2050 <sup>1</sup>. This population should be supplied with two basic  
44 commodities: water and energy. Energy demands for conventional water and wastewater  
45 processes are a significant part of the problem in supplying these commodities; e.g., in the  
46 US, approximately 5% of the electricity consumption is due to the water treatment processes  
47 <sup>2</sup>. Renewable energy sources represent some of the most appropriate options to reach the  
48 sustainable energy production objective <sup>3,4</sup>. In addition, the development of processes that can  
49 use microorganisms to produce electricity from wastes represents an interesting approach for  
50 bioenergy production <sup>5</sup>. On the one hand, microorganisms are not as selective and sensitive as  
51 the chemical catalysts, and hence, the spectrum and quality of the potential fuels to be used  
52 can be expanded with the use of microorganisms, relative to chemical catalysts. In addition,  
53 microorganisms are self-replicating, and consequently, the catalyst for the substrate oxidation  
54 is self-sustaining. On the other hand, wastewaters contains a significant amount of organic  
55 pollutants <sup>6</sup>. Unfortunately, the large number of constituents and dilute nature makes it very  
56 difficult to extract the chemical energy contained in waste <sup>7</sup>; hence, biotechnological  
57 processes that tend to function well under dilute circumstances represent an option for its  
58 energetic valorization.

59 Microbial Fuel Cells (MFCs) are electrochemical devices able to extract the chemical energy  
60 contained in a fuel by means of microbial metabolisms <sup>8</sup>. However, in spite of the importance  
61 of the influent COD concentration on the microbial metabolisms, little information can be  
62 found in the literature related to its influence on MFC performance. The COD concentration  
63 effects are of great importance in the practical application of MFCs in both the short term and

64 the long term, because the COD concentration profiles of the domestic wastewaters change  
65 due to daily and seasonal changes<sup>9, 10</sup>. Domestic wastewaters are one of the main fuels used  
66 in MFC because of its widespread availability and its COD content<sup>11</sup>.

67 **In the long term, the importance of the COD concentration profiles is related to the**  
68 **composition of the microbial community.** These changes are very important because full-scale  
69 MFCs operate with mixed cultures, combining electrogenic microbes **such as *Geobacter* and**  
70 ***Shewanella* with non electrogenic microbes such as *Bacteroidia*, *Clostridia*, *Bacilli*,**  
71 ***Lactobacillales*, etc.**<sup>12</sup>. The use of mixed cultures is justified by the results of studies in which  
72 **mixed cultures were shown to have power densities that were similar to those observed in**  
73 **pure culture experiments**<sup>13</sup>. Moreover, the use of mixed cultures reduces the operating costs  
74 and allows the system to use low-quality fuels, such as wastewaters<sup>14</sup>.

75 Regarding the COD influence over the microbial population, on the one hand, the increase of  
76 the influent COD concentration **reduces the competition for the substrate**, allowing for the  
77 development of a wide spectrum of microorganisms. On the other hand, low COD  
78 concentrations lead to a competition between microorganisms for the substrate, with only the  
79 most adapted to the environmental conditions prevailing<sup>15</sup>. In this sense, the low COD  
80 concentrations are more selective for the microbial population than the high COD  
81 concentrations<sup>12, 14</sup>. **In general, electrogenic organisms present lower growth rates. In the**  
82 **particular case of *Geobacter*, it has been reported<sup>16</sup> that a maximum growth rate of 2.4 d<sup>-1</sup> can**  
83 **occur whereas non electrogenic microorganisms such as *Clostridia* presents maximum**  
84 **specific growth rate of 3.3 d<sup>-1</sup><sup>17, 18</sup>. However, under substrate limitations *Geobacter* growth**  
85 **was faster due to its higher substrate affinity**<sup>19</sup>.

86 These changes in the microbial populations in the MFC could affect not only the COD  
87 removal rates but also the electrochemical performance of the MFC<sup>20</sup>. In the particular case

88 of the MFC, reporting the CE is sufficient to evaluate its performance as an electrochemical  
89 power system based on wastes as fuel <sup>2</sup>.

90 The use of mixed cultures reduces the operational costs and enhances the adaptive capacity  
91 due to microbial diversity. These characteristics lead to an improved capacity to degrade  
92 mixed substrates and the possibility of continuous processing, which is quite interesting when  
93 operating with an MFC.

94 In this context, the goal of this work was to assess the long-term influence of a transient  
95 change of the influent organic concentration on the performance of MFC. To accomplish this  
96 goal, a MFC seeded with a mixed culture was used. Once started-up and acclimated, the MFC  
97 was subjected to transient COD concentrations, and then, the long-term effects on COD  
98 removal and current exerted were monitored. The results are discussed in light of the present  
99 knowledge of the technology, and they are of great interest because the operation of MFCs in  
100 actual application would be under these changing conditions.

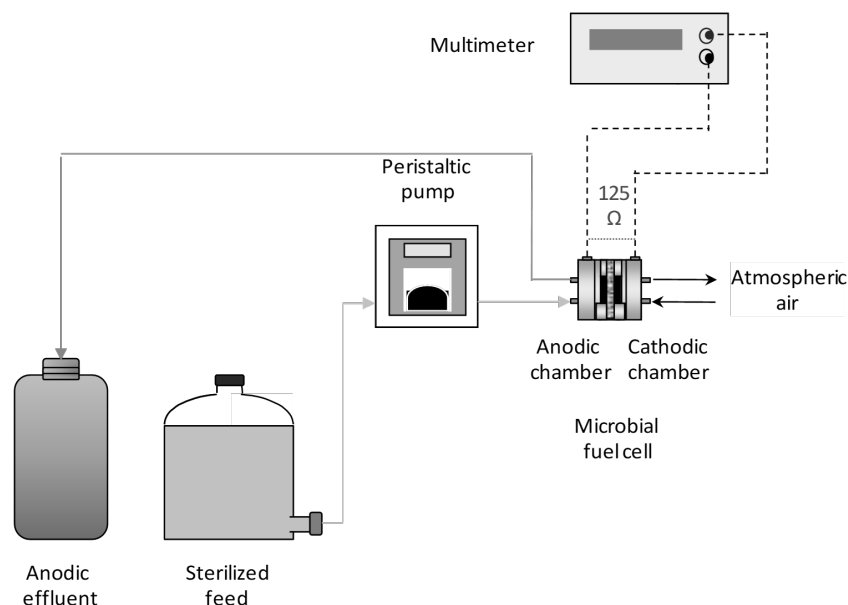
101

## 102 **2. Experimental Procedure**

### 103 **2.1 Experimental set-up**

104 The experimental micro-scale set-up used in this work consisted of a two-chambered micro-  
105 scale MFC, as described elsewhere <sup>21</sup>. The anodic and cathodic electrodes were based on  
106 Toray carbon papers TGPH-120 (E-TEK, USA): the anodic electrode had a Teflon content of  
107 20 %, and the cathodic one had a Teflon content of 10 %. In the cathode, a catalytic layer with  
108 0.5 mg Pt/cm<sup>2</sup> loading was deposited onto a microporous layer. The anodic and cathodic  
109 chambers were built on a graphite plate. Both chambers were separated by a Sterion<sup>®</sup>  
110 membrane. The active area of the anodic chamber was 4.65 cm<sup>2</sup>, and its volume was 0.95  
111 cm<sup>3</sup>. The active area of the cathodic chamber was 2.85 cm<sup>2</sup>, and its volume was 0.50 cm<sup>3</sup>. The  
112 membrane-electrode assembly was performed according to the literature <sup>22</sup>. An air breathing

113 cathode was used. Air-breathing systems use free convection airflow to supply oxygen to the  
114 cathode. This air breathing cathode is a very robust cathode, as reported in the literature <sup>21</sup>.  
115 A schematic view of the set-up is shown in Figure 1.



116  
117 Figure 1. Schematic view of the set-up.  
118

119 The MFC was operated in continuous mode. The anodic compartment of the MFC was fed  
120 from a wastewater reservoir 800 mL in capacity. A peristaltic pump was used for feeding the  
121 wastewater from the reservoir to the anodic chamber of the MFC at a flow rate of 0.5  
122 mL/min. To avoid the degradation of the wastewater during its storage, the wastewater was  
123 sterilised for 20 min at 120 °C. The anodic chamber of the MFCs was seeded two days after  
124 the start-up of the MFCs with a *Geobacter* enriched mixed culture taken from the effluent of a  
125 working MFC <sup>23</sup>. In this way, the absence of electricity generation before the seeding of the  
126 MFC was verified, with these data serving as abiotic control data.

127 The composition of the synthetic wastewater used in the experiments is presented in Table 1.

128 The main organic substrate was glucose because it is often used as a model substrate <sup>24, 25</sup>.

129 The trace minerals concentration was always maintained constant, whereas the organic COD

130 concentration was increased at the values of 300 mg/L, 900 mg/L, and 1800 mg/L,

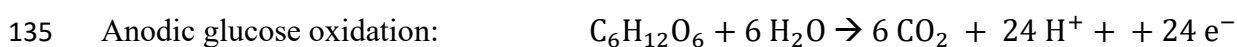
131 corresponding to n, 3n, and 6n COD concentrations, respectively.

132 **Table 1.** Synthetic wastewater composition.

<b>Compound</b>	<b>Concentration n</b>	<b>Concentration 3n</b>	<b>Concentration 6n</b>
Glucose (mg/l)	300	900	1800
(NH <sub>4</sub> ) <sub>2</sub> SO <sub>4</sub> (mg/l)	74.2	74.2	74.2
KH <sub>2</sub> PO <sub>4</sub> (mg/l)	44.5	44.5	44.5
NaHCO <sub>3</sub> (mg/l)	115	115	115
MgSO <sub>4</sub> ·7H <sub>2</sub> O (mg/l)	50	50	50
CaCl <sub>2</sub> (mg/l)	30	30	30
(NH <sub>4</sub> ) <sub>2</sub> Fe(SO <sub>4</sub> ) <sub>2</sub>	3	3	3

133

134 The primary reactions occurring in the MFC were the following ones:



138 The standard potential value,  $E_{emf}^0$ , of the glucose oxidation is 0.104 V vs. **Normal Hydrogen**  
 139 **Electrode (NHE)** and 1.229 V vs. NHE for the oxygen reduction reaction<sup>26</sup>. These values can  
 140 be modified when changing the operational conditions. As a result, the actual potentials can  
 141 be determined according to the Nernst Equation.

142 
$$E_{emf} = E_{emf}^0 - \frac{R \cdot T}{n \cdot F} \ln(\Pi) \quad (1)$$

143 where

144  $E_{emf}$  is the actual potential

145 R is the universal gas constant

146 T is the absolute temperature

147 n is the number of moles of electrons transferred in the cell reaction or half-reaction

148 F is the Faraday constant

149  $\Pi$  is the reaction quotient.

150

151 In the Nernst equation, it can be observed that the higher the reactant concentration, the higher  
152 the exerted potential. The whole cell potential can be calculated as the difference between the  
153 cathodic and anodic half cell potentials.

$$154 \quad E_{\text{emf}} = E_{\text{cat}} - E_{\text{an}} \quad (2)$$

155 However, the cell potential not only depends on electrolyte concentration but also on over  
156 potentials and Ohmic losses<sup>27</sup>. Thus, the actual cell potential can be determined using eq. 3:

$$157 \quad E_{\text{cell}} = E_{\text{emf}} - (\sum \eta_a + |\sum \eta_c| + IR\Omega) \quad (3)$$

158 where

159  $\sum \eta_a$  and  $|\sum \eta_c|$  are the cathodic and anodic overpotentials, respectively

160  $IR\Omega$  is the sum of the Ohmic losses, which are proportional to the generated current (I) and  
161 Ohmic resistance of the system ( $R\Omega$ ).

162 During normal operation, the anode and the cathode were connected by means of copper  
163 wires and a resistor (125  $\Omega$ ). The potentials between the edges of this resistor were  
164 continuously monitored. These potentials are directly related to the current flowing between  
165 the electrodes by Ohms law (eq. 4).

$$166 \quad I_{\text{MFC}} = \frac{E_{\text{cat}} - E_{\text{an}} - (\sum \eta_a + |\sum \eta_c| + IR\Omega)}{125} \quad (4)$$

167 where  $I_{\text{MFC}}$  is the intensity of the electrical current exerted by the MFC.

168 In the set-up used in this work, electrical current was generated due to organic matter  
169 oxidation. This oxidation was monitored by measuring the parameter of the COD removal  
170 rate ( $r_{\text{COD}}$ ). This parameter can be calculated, once steady state is achieved, according to eq. 5,  
171 where  $Q$  is the influent flow rate to the anodic chamber, and  $\Delta\text{COD}$  is the COD removed from  
172 this stream.

$$173 \quad r_{\text{COD}} = Q \cdot \Delta\text{COD} \quad (5)$$



174 The relationship between the COD removal rate and the theoretical current intensity can be  
 175 determined by taking into account the stoichiometry of the oxidation of the COD, for which  
 176 every mmol of COD corresponds to 4 mmol of e<sup>-</sup>, as represented in the following equation  
 177 with (n), as well as the Faraday constant (96485 C mol<sup>-1</sup> e<sup>-</sup>), the molar mass of oxygen (M)  
 178 and the COD removal rate (r<sub>COD</sub>). This relationship is presented in eq. 6.

$$179 \quad I(\text{mA}) = \frac{n(4 \text{ mmol e}^- \cdot \text{mmol}^{-1} \text{ O}_2) \cdot F(964854 \text{ mC} \cdot \text{mmol e}^-) \cdot r_{\text{COD}}(\text{mg O}_2 \cdot \text{d}^{-1})}{M(\text{mg O}_2 \cdot \text{mmol}^{-1} \text{ O}_2) \cdot 86400(\text{s} \cdot \text{d}^{-1})} \quad (6)$$

180 Therefore, the CE is defined as the ratio of total quantity of Coulombs actually transferred  
 181 from the substrate to the anode, to the maximum possible Coulombs transferred if all the  
 182 substrate removal generated current. High CE values are desirable for increasing energy  
 183 recovery. The CE can be calculated integrating over time the Coulombs actually transferred  
 184 divided by the stoichiometric theoretical value (eq. 7).

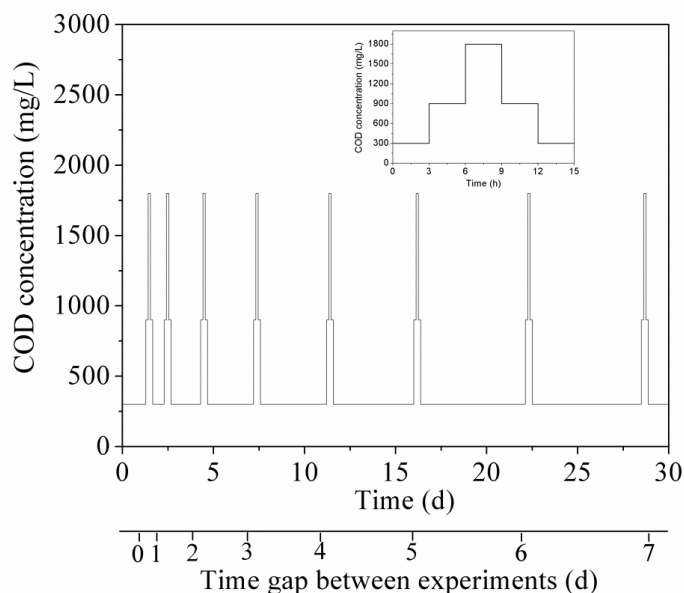
$$185 \quad \text{CE} = \frac{M \cdot \int_0^t I \cdot dt}{n \cdot F \cdot V_{\text{anodic}} \cdot r_{\text{COD}}} \quad (7)$$

186

## 187 2.2 Methodology

188 To determine the long-term effect of transient COD concentrations, the influent COD was  
 189 step-wise modified from 300 mg/l to 1800 mg/L. This step-wise modification was repeated by  
 190 changing the time gaps (see Figure 2). The effects were studied in a time period ranging from  
 191 1 to 7 days. **The perturbation intervals were selected based on the perturbations experienced**  
 192 **in a conventional wastewater treatment plant**<sup>10</sup>. These plants are subjected to daily and  
 193 weekly changes, which could affect the performance of the facility<sup>10, 28</sup>. As it is well known,  
 194 one of the main applications of the microbial fuel cell is wastewater treatment combined with  
 195 clean energy generation. As a result, we were interested in evaluating the influence of the  
 196 perturbations for periods ranging from 1 to 7 days on the performance of the microbial fuel

197 cell. A description of the procedure is presented in Figure 2. During the transient COD  
198 changes and afterwards, the main operational parameters were determined.  
199



200  
201 Figure 2. Schematic view of the experimental procedure. Inset: close-up of the step-wise  
202 transient COD modifications.

### 204 2.3 Characterization techniques

205 The quantities of the total suspended solid and the COD were measured according to  
206 processes reported in the literature<sup>29</sup>. The conductivity, dissolved oxygen, and pH were  
207 measured by means of a LF538 WTW conductivity-meter, an Oxi538 WTW oxy-meter, and a  
208 GLP22 Crison pH-meter, respectively. A digital multi-meter was connected to the system to  
209 continuously monitor the value of the cell potential. Polarization curves were recorded using  
210 an Autolab PGSTAT 30 potentiostat/galvanostat (Ecochemie, the Netherlands).

211 Polarization curves provide interesting information about the operating conditions of the  
212 MFC, particularly about the actual capabilities of the MFC. These curves allow us to discern  
213 three important parameters: the open circuit voltage (OCV) or the maximum allowable MFC

214 voltage (for a nil current), the maximum intensity reachable (for a nil potential) and the  
215 maximum feasible power density. In addition, the shape of the curve provides information  
216 about the limiting stage, which controls the performance of the cell.

217 Typically, the shape of the polarization curve can be divided into three zones, which can be  
218 explained by the three major sources of loss of the fuel cells: the activation losses, voltage  
219 loss due to Ohmic loss, and voltage loss due to concentration loss.

220 In MFCs, linear polarization curves are most often obtained <sup>2,30</sup> because, in most MFC  
221 devices, the operation mainly occurs in the Ohmic region of the curve <sup>2</sup>.

222 **The presence of the *Geobacter* and *Clostridia* genus were detected by MALDI-TOFF**  
223 **fingerprints. The matrix solutions were prepared by saturation of cyano-4-hydroxycinnamic**  
224 **acid in 1: 48:2 acetonitrile: water: trifluoroacetic acid matrix solution. The microorganisms**  
225 **were sterilized with ethanol at 75%. The solution was centrifuged (1000 rpm) for ten minutes**  
226 **and the supernatant removed. The microorganism was then extracted from the precipitate**  
227 **using 20  $\mu$ L of acetonitrile/formic acid/water (50:35:15).**

228

### 229 **3. Results and discussion**

230 The system was continuously operated for more than two months in order to ensure operation  
231 under steady-state conditions. Once the steady state was achieved, the culture was  
232 characterized being the main communities *Geobacter* and *Clostridia*, and then the transient  
233 COD tests were performed. These tests consisted of the modification of the influent organic  
234 COD concentration fed to the MFC. The transient modifications were maintained for 12  
235 hours, and the effects were evaluated for up to 7 days. The experiments were performed at  
236 constant flow rates by modifying the influent COD but not the hydraulic retention time.  
237 During these tests, the remaining operational conditions were kept constant. The COD  
238 concentrations tested were the following: the COD concentration feed to the system under

239 steady state (used as the control value and named “n”), three times the control concentration  
240 (named as 3n) and six times the control concentration (named as 6n). To study the possible  
241 hysteresis of the system, when modifying the influent COD concentration, the forward scan  
242 was complemented with a reverse scan.

243 It is important to remark that similar trends, but with different values, were observed for the  
244 main parameters in each transient COD test.

### 245 **3.1. Long-term effect on the COD removal**

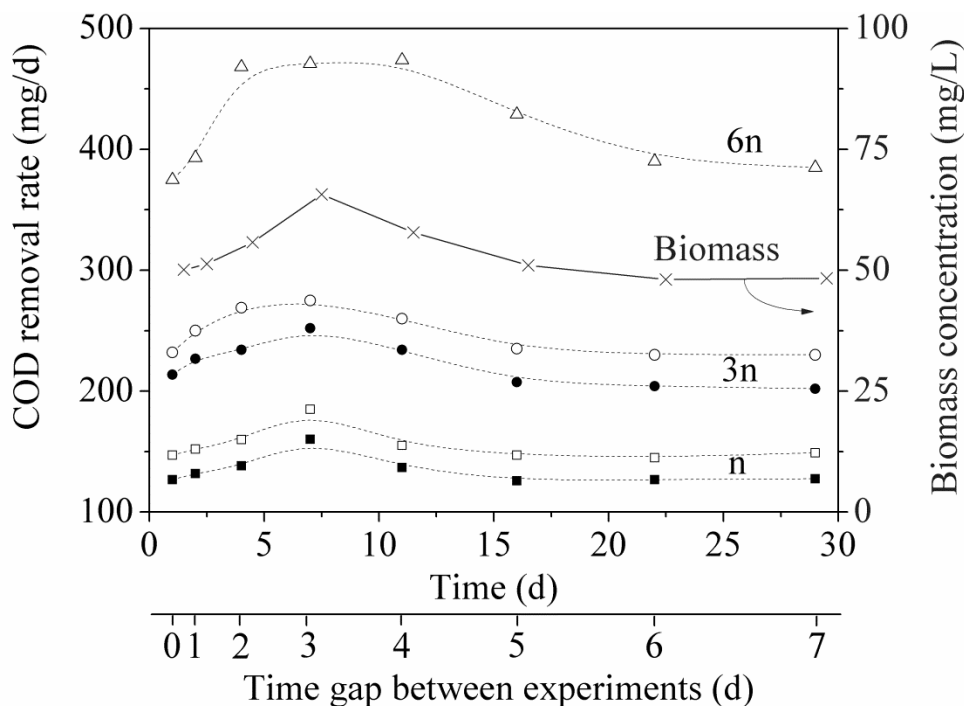
246 Regarding the COD removal, it must be noted that the values obtained in the forward and  
247 reverse scans were found to be different. The values obtained in the reverse scans are  
248 represented by the corresponding symbols for the forward scans but with open characters.

249 During the step-wise procedure, the highest concentration, 6n, was studied once, and  
250 therefore, no reverse scan is presented.

251 In Figure 3, the COD removal rates versus the time break between experiments are presented.

252 This figure shows two different behaviors. In the first stage, with a time gap of 3 or lower  
253 than 3 days, the system showed increasing COD degradation rates when it was subjected to  
254 transient modifications in the influent COD concentration. The increase in the degradation  
255 rate presented a gentle slope when operating at the low COD concentrations of the n series,  
256 but a very stepped slope when the system was operated at the highest COD concentrations of  
257 the 6n series. In the case of the highest influent COD concentrations, the enhancement of the  
258 COD degradation rate was higher than 20% and could be caused by the increase of the  
259 biomass concentration on the surface of the anodic electrode due to the transient exposition to  
260 high COD concentrations<sup>23</sup>. To corroborate the biomass growth, the biomass concentration in  
261 the effluent wastewater was determined. The values obtained are presented in Fig. 3. The  
262 trend was very similar to that obtained for the COD removal rate, indicating a direct  
263 relationship between them. As shown in Fig 3, when several transient modifications occurred

264 in a short period of time the enhancement was more evident, suggesting an accumulative  
 265 effect. The highest response was obtained when the time gap between transient COD tests  
 266 was 3 days. When operating with longer time gaps ranging between 4 and 7 days, the  
 267 behavior of the systems was different, decreasing the COD removal rate when increasing the  
 268 time gap. This reduction of the COD removal rate could be explained by the decay of the  
 269 excess of biomass grown when the MFC was exposed to high COD concentrations.  
 270 According to literature this reduction presents a linear trend <sup>31</sup>, this trend can also be observed  
 271 in the biomass concentration data presented on Figure 3. These results verify that the MFCs  
 272 behave in different ways, depending on the events that occurred a few days prior. For longer  
 273 time gaps between the experiments (higher than 7 days), the system reached a similar  
 274 response to that obtained before the tests, indicating that after 7 days, the system was no  
 275 longer influenced by the previous events and behaves as usual.



276  
 277 Figure 3. COD removal rates versus time and versus the time gap between experiments. Full and  
 278 open symbols correspond to the forward and reverse scans, respectively. Crosses correspond to  
 279 the effluent biomass concentration.

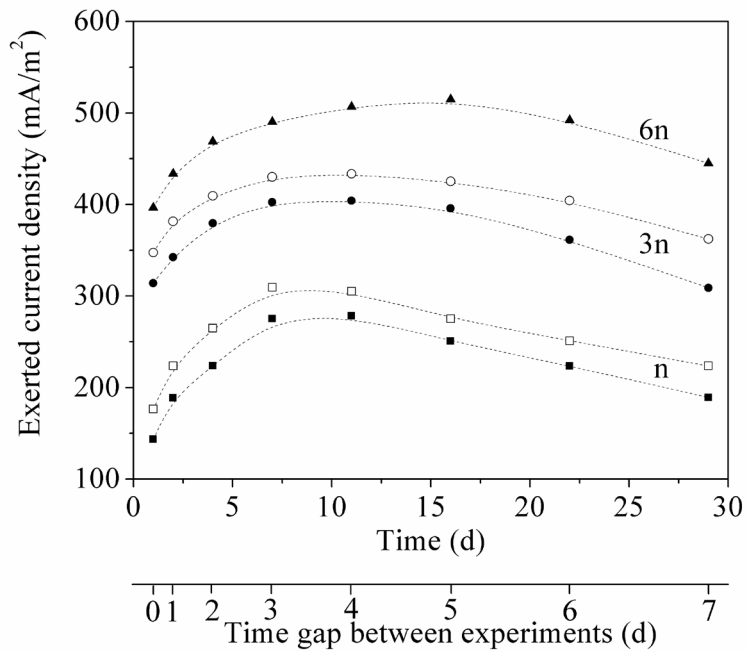
280

### 281 **3.2. Long-term effect on the current density generation and the CE**

282 Regarding the exerted current density, the obtained results are shown in Figure 4, where the  
283 values obtained in the reverse scans are represented by the corresponding symbol for the  
284 forward scan, but with open characters.

285 In this figure, two stages are also shown. However, the exerted current densities presented an  
286 opposite trend to that obtained when studying the COD removal rate. In the case of the  
287 exerted current density, the trend was more stepped when low COD concentrations were  
288 studied, presenting a maximum between 3 and 4 days of time gap between experiments,  
289 depending on the COD concentration. The control experiment, n, and three times the COD  
290 concentration, 3n, reached the maximum after 3 days, whereas the experiment with six times  
291 the COD concentration, 6n, reached the maximum after 4 days.

292 Subsequently, the current density generations of the 3n and 6n tests decay, reaching a value  
293 similar to that obtained at the beginning of the tests when the time gap between experiments  
294 was 7 days. However, in the case of the n test, the exerted current density remained higher  
295 than that obtained at the beginning of the tests, even after 7 days, presenting an increase in the  
296 exerted current density of approximately 15%. This phenomenon could be related to the  
297 enhancement of the electrogenic population, with this enhancement being maintained even  
298 when the influent COD concentration was reduced. This behavior could be explained by a  
299 higher affinity of *Geobacter* microorganisms for the substrate than that of the non-  
300 electrogenic organisms<sup>16, 32</sup>. Therefore, when the influent COD concentration is reduced, the  
301 *Geobacter* outcompete the non-electrogenic ones because of the lower affinity for the  
302 substrates of the latter microbial group.



303

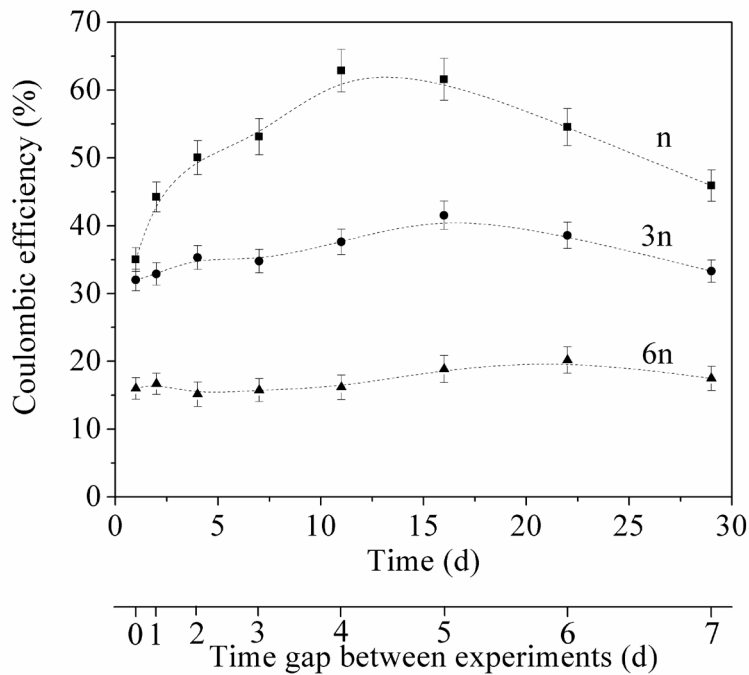
304 Figure 4. Exerted current density versus the time gap between experiments. Full and open

305 symbols correspond to the forward and reverse scans, respectively.

306

307 Because of the different trends in the COD removal rate and the current density generation,  
 308 changes in the CE with time were expected. The determined CE values are shown in Figure 5,  
 309 where the error bars correspond to measurement replicates. This figure shows that the trend  
 310 of the CE highly depended on the COD concentration tested. In the case of the highest  
 311 concentrations, i.e., 3n and 6n, the CE was almost independent of the time gap between  
 312 experiments. This behavior could be related to a compensated development of both  
 313 electrogenic and not-electrogenic microorganisms. In these cases, the COD concentration is  
 314 very high and allows the development of both types of microbial populations, electrogenic  
 315 and not-electrogenic, without limitations. The compensated growth when no limitations occur  
 316 indicated that the growth rate of both groups were very similar. However, in the case of the  
 317 lowest COD concentration, n, the CE was clearly influenced, ranging between 35 and 65%.  
 318 This behavior could be explained because of the combined effect of the higher substrate  
 319 affinity of *Geobacter* for the substrate and because of the biomass growth rate of electrogenic

320 and non-electrogenic microorganisms. In this case, when the COD concentration is scarce, the  
 321 *Geobacter* microorganisms prevailed, and the MFC culture was enriched in electrogenic  
 322 microorganisms, leading to a better electrochemical performance. In the case of the lower  
 323 COD concentration, the enhancement of the CE was maintained up to 4 days.  
 324



325  
 326 Figure 5. CE versus the time and time gap between experiments.

327

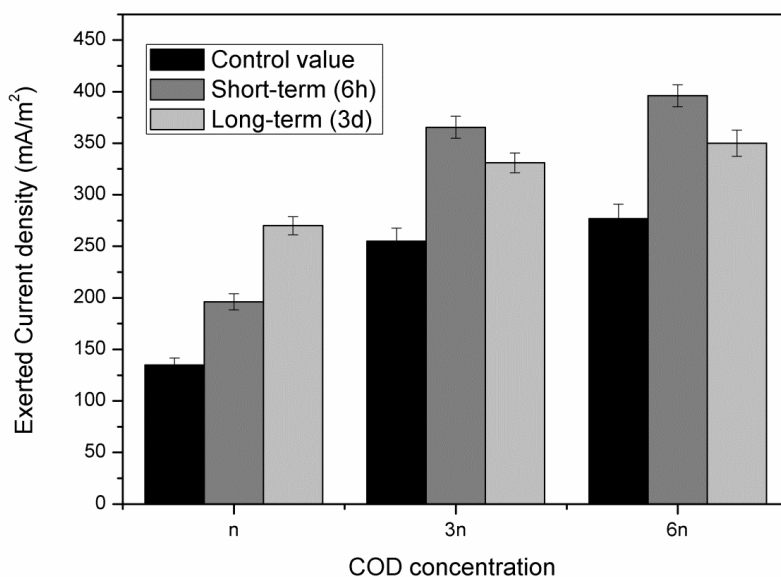
### 328 3.4. Short and long-term effect comparison

329 To compare and evaluate the differences in the exerted current density in the short and long-  
 330 term, both results are presented in Figure 6. Data for the short-term effects were taken from  
 331 the literature<sup>23</sup>. In Figure 6, the current density exerted during the steady state as well as the  
 332 values reached after the transient COD modification in the short-term, after 6 h, and long-  
 333 term, after 3 d, are presented.

334 In this figure, it can be seen that the exerted current obtained when operating at low COD  
 335 loading rates presented an increasing trend in the short term and in the long term. The



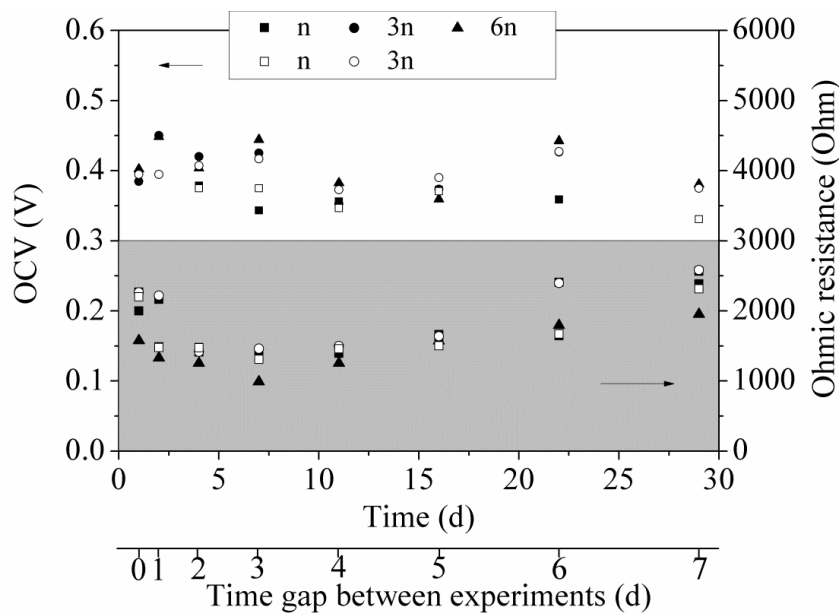
336 enhancement in the long term could be explained because of the enrichment in *Geobacter*  
337 microorganisms in the culture after the repetitive transient COD modifications. However,  
338 when working at the highest loads, COD concentrations 3n and 6n, the system showed a  
339 higher enhancement at the short term than at the long term. This behavior could be explained  
340 because of the enrichment of the non-electrogenic organisms in the microbial culture when  
341 working with high COD concentrations. Under these conditions, a significant amount of  
342 acetate could be produced from the glucose fermentation by *Clostridia*. Then, some of the  
343 acetate could be consumed by *Geobacter*<sup>33</sup>. These results are in accordance with the higher  
344 affinity of the *Geobacter* microorganisms for the substrate<sup>16</sup>, which leads to better  
345 electrogenic performance when operating at low COD concentrations.



346  
347 Figure 6. Exerted current density versus COD concentration in the short-term and the long-term.

348  
349 Finally, to characterize the electrochemical abilities of the system the polarization curves were  
350 performed. From the obtained results, the Open Circuit Voltages (OCVs) and the Ohmic  
351 resistance values were determined. The white area of Fig. 7 shows the OCV values obtained  
352 in different stress tests performed on the system.

353



354

355

356 Figure 7. Open circuit voltage and Ohmic resistance obtained during the COD stress tests. Full  
357 and open symbols correspond to the forward and reverse scans, respectively.

358

359 It can be seen that the response was kept constant, in spite of the COD concentration. This  
360 behavior can be explained by the fact that the OCV only depends on the potential difference  
361 between the electrodes. As is known, the potential of an electrode is a function of the oxidation  
362 and reduction reactions, but not of the extension of the reaction<sup>34</sup>. The stability of the chemical  
363 reactions, and therefore of the OCV, indicates that the electrogenic microbial population located  
364 at the anodic compartment did not change significantly during the experiments<sup>23</sup> being the most  
365 important group *Geobacter*. Regarding the Ohmic resistance, its values are presented in the grey  
366 area of Fig. 7. This figure shows that the values initially presented a descending trend. This  
367 behavior could be explained by the development of a more active electrogenic biofilm at the  
368 surface of the electrode<sup>3</sup>. In this case, the higher activity reduced the resistance to the  
369 electrical current. However, when the time between transient modifications was increased, the  
370 Ohmic resistance also increased, which could be explained because of the decay of the

371 *Geobacter* microorganisms that had previously grown. The average value of the sum of the  
372 overpotentials experienced was approximately 0.07 V.

373

#### 374 **4. Conclusions**

375 From the results obtained in this paper, the following conclusions were made.

376 The time dependence experienced in the electrogenic behavior of the MFC makes these devices  
377 sensitive to transient COD concentrations. This time dependence can be explained by changes in  
378 the microbial population and the metabolisms while the electrochemical performance remains  
379 almost constant. This behavior is very interesting for the potential application of MFCs as  
380 bioelectrochemical sensors. Modifications in the COD loading rate maintained during 12 hours  
381 caused long-term modifications in the microbiological behavior of the cell, increasing the ability  
382 of the microorganisms to degrade the COD. The main effects were observed during the first 4  
383 days, although the influence was identified up to 7 days.

384 Note that the electrochemical behavior of the cell was also affected. In the long term, the  
385 Coulombic efficiency decreased when the system was exposed to higher COD loading. In this  
386 case, the effects were significant for at least 7 days.

387 Finally, it was also observed that the *Geobacter* microorganisms presented higher affinity for the  
388 substrate than the non-electrogenic organisms. This higher affinity leads to better results when  
389 working with low COD concentrations, which is a very important finding for enhancement of the  
390 population of electrogenic microorganisms in a mixed culture MFC.

391

#### 392 **Acknowledgements**

393 Authors thanks the Spanish Government for the financial support thorough the Project  
394 CTQ2013-49748-EXP.

395

- 397 1. Ruane, J.; Sonnino, A., Agricultural biotechnologies in developing countries and their possible  
398 contribution to food security. *Journal of Biotechnology* **2010**, 156, (4), 356-363.
- 399 2. Logan, B. E.; Hamelers, B.; Rozendal, R.; Schröder, U.; Keller, J.; Freguia, S.; Aelterman, P.;  
400 Verstraete, W.; Rabaey, K., Microbial fuel cells: Methodology and technology. *Environmental Science*  
401 *and Technology* **2006**, 40, (17), 5181-5192.
- 402 3. Mateo, S.; Gonzalez del Campo, A.; Cañizares, P.; Lobato, J.; Rodrigo, M. A.; Fernandez, F. J.,  
403 Bioelectricity generation in a self-sustainable Microbial Solar Cell. *Bioresource Technology* **2014**, 159,  
404 451-454.
- 405 4. Borole, A. P.; Hamilton, C. Y.; Aaron, D. S.; Tsouris, C., Investigating microbial fuel cell  
406 bioanode performance under different cathode conditions. *Biotechnology Progress* **2009**, 25, (6),  
407 1630-1636.
- 408 5. Premier, G. C.; Kim, J. R.; Massanet-Nicolau, J.; Kyazze, G.; Esteves, S. R. R.; Penumathsa, B. K.  
409 V.; Rodríguez, J.; Maddy, J.; Dinsdale, R. M.; Guwy, A. J., Integration of biohydrogen, biomethane and  
410 bioelectrochemical systems. *Renewable Energy* **2013**, 49, 188-192.
- 411 6. Buendía, I. M.; Fernández, F. J.; Villaseñor, J.; Rodríguez, L., Biodegradability of meat industry  
412 wastes under anaerobic and aerobic conditions. *Water Research* **2008**, 42, (14), 3767-3774.
- 413 7. Pinto, R. P.; Srinivasan, B.; Manuel, M. F.; Tartakovsky, B., A two-population bio-  
414 electrochemical model of a microbial fuel cell. *Bioresource Technology* **2010**, 101, (14), 5256-5265.
- 415 8. Zhang, X.; He, W.; Ren, L.; Stager, J.; Evans, P. J.; Logan, B. E., COD removal characteristics in  
416 air-cathode microbial fuel cells. *Bioresource Technology* **2015**, 176, 23-31.
- 417 9. Wang, H. Y.; Bernarda, A.; Huang, C. Y.; Lee, D. J.; Chang, J. S., Micro-sized microbial fuel cell:  
418 A mini-review. *Bioresource Technology* **2011**, 102, (1), 235-243.
- 419 10. Tchobanoglous, G.; Burton, F. L.; Metcalf; Eddy, *Wastewater engineering : treatment,*  
420 *disposal, and reuse.* McGraw-Hill: New York, 1991.
- 421 11. Liu, H.; Ramnarayanan, R.; Logan, B. E., Production of Electricity during Wastewater  
422 Treatment Using a Single Chamber Microbial Fuel Cell. *Environmental Science and Technology* **2004**,  
423 38, (7), 2281-2285.
- 424 12. Ishii, S.; Suzuki, S.; Norden-Krichmar, T. M.; Phan, T.; Wanger, G.; Neelson, K. H.; Sekiguchi, Y.;  
425 Gorby, Y. A.; Bretschger, O., Microbial population and functional dynamics associated with surface  
426 potential and carbon metabolism. *ISME Journal* **2014**, 8, (5), 963-978.
- 427 13. Tartakovsky, B.; Guiot, S. R., A comparison of air and hydrogen peroxide oxygenated  
428 microbial fuel cell reactors. *Biotechnology Progress* **2006**, 22, (1), 241-246.
- 429 14. Kleerebezem, R.; van Loosdrecht, M. C., Mixed culture biotechnology for bioenergy  
430 production. *Current Opinion in Biotechnology* **2007**, 18, (3), 207-212.
- 431 15. Temudo, M. F.; Kleerebezem, R.; Van Loosdrecht, M., Influence of the pH on (Open) mixed  
432 culture fermentation of glucose: A chemostat study. *Biotechnology and Bioengineering* **2007**, 98, (1),  
433 69-79.
- 434 16. Picioreanu, C.; Head, I. M.; Katuri, K. P.; van Loosdrecht, M. C. M.; Scott, K., A computational  
435 model for biofilm-based microbial fuel cells. *Water Research* **2007**, 41, (13), 2921-2940.
- 436 17. Fernández-Morales, F. J.; Villaseñor, J.; Infantes, D., Modeling and monitoring of the  
437 acclimatization of conventional activated sludge to a biohydrogen producing culture by biokinetic  
438 control. *International Journal of Hydrogen Energy* **2010**, 35, (20), 10927-10933.
- 439 18. Infantes, D.; González del Campo, A.; Villaseñor, J.; Fernández, F. J., Kinetic model and study  
440 of the influence of pH, temperature and undissociated acids on acidogenic fermentation. *Biochemical*  
441 *Engineering Journal* **2012**, 66, 66-72.
- 442 19. Picioreanu, C.; Katuri, K. P.; Head, I. M.; Van Loosdrecht, M. C. M.; Scott, K., Mathematical  
443 model for microbial fuel cells with anodic biofilms and anaerobic digestion. In *Water Science and*  
444 *Technology*, 2008; Vol. 57, pp 965-971.

- 445 20. Zhang, Y.; Min, B.; Huang, L.; Angelidaki, I., Electricity generation and microbial community  
446 response to substrate changes in microbial fuel cell. *Bioresource Technology* **2011**, 102, (2), 1166-  
447 1173.
- 448 21. Mateo, S.; Rodrigo, M.; Fonseca, L. P.; Cañizares, P.; Fernandez-Morales, F. J., Oxygen  
449 availability effect on the performance of air-breathing cathode microbial fuel cell. *Biotechnology*  
450 *Progress* **2015**.
- 451 22. Gonzalez Del Campo, A.; Cañizares, P.; Lobato, J.; Rodrigo, M. A.; Fernandez, F. J., Electricity  
452 production by integration of acidogenic fermentation of fruit juice wastewater and fuel cells.  
453 *International Journal of Hydrogen Energy* **2012**, 37, (11), 9028-9037.
- 454 23. Gonzalez del Campo, A.; Lobato, J.; Cañizares, P.; Rodrigo, M. A.; Fernandez Morales, F. J.,  
455 Short-term effects of temperature and COD in a microbial fuel cell. *Applied Energy* **2013**, 101, 213-  
456 217.
- 457 24. Fernández, F. J.; Castro, M. C.; Villasenor, J.; Rodríguez, L., Agro-food wastewaters as external  
458 carbon source to enhance biological phosphorus removal. *Chemical Engineering Journal* **2011**, 166,  
459 (2), 559-567.
- 460 25. Bonfatti, F.; Ferro, S.; Lavezzo, F.; Malacarne, M.; Lodi, G.; De Battisti, A., Electrochemical  
461 incineration of glucose as a model organic substrate II. Role of active chlorine mediation. *Journal of*  
462 *the Electrochemical Society* **2000**, 147, (2), 592-596.
- 463 26. Liu, H.; Logan, B. E. In *Electricity generation using an air-cathode single chamber microbial*  
464 *fuel cell (MFC) in the absence of a proton exchange membrane*, ACS, Division of Environmental  
465 Chemistry - Preprints of Extended Abstracts, 2004; 2004; pp 1485-1488.
- 466 27. Osman, M. H.; Shah, A. A.; Walsh, F. C., Recent progress and continuing challenges in bio-fuel  
467 cells. Part I: Enzymatic cells. *Biosensors and Bioelectronics* **2011**, 26, (7), 3087-3102.
- 468 28. Fernandez, F. J.; Seco, A.; Ferrer, J.; Rodrigo, M. A., Use of neurofuzzy networks to improve  
469 wastewater flow-rate forecasting. *Environmental Modelling and Software* **2009**, 24, (6), 686-693.
- 470 29. American Public Health Association.; American Water Works Association.; Water Pollution  
471 Control Federation.; APHA.; AWWA.; APCF., *Standard methods for the examination of water and*  
472 *wastewater*. 14th ed.; Washington, D.C.,, 1989; p 1193 s.
- 473 30. Fan, Y.; Sharbrough, E.; Liu, H., Quantification of the Internal Resistance Distribution of  
474 Microbial Fuel Cells. *Environmental Science & Technology* **2008**, 42, (21), 8101-8107.
- 475 31. Batstone, D. J.; Keller, J.; Angelidaki, I.; Kalyuzhnyi, S. V.; Pavlostathis, S. G.; Rozzi, A.; Sanders,  
476 W. T.; Siegrist, H.; Vavilin, V. A., The IWA Anaerobic Digestion Model No 1 (ADM1). *Water Science and*  
477 *Technology* **2002**, 45, (10), 65-73.
- 478 32. Kovárová-Kovar, K.; Egli, T., Growth kinetics of suspended microbial cells: From single-  
479 substrate- controlled growth to mixed-substrate kinetics. *Microbiology and Molecular Biology*  
480 *Reviews* **1998**, 62, (3), 646-666.
- 481 33. de los Ángeles Fernandez, M.; de los Ángeles Sanromán, M.; Marks, S.; Makinia, J.; Gonzalez  
482 del Campo, A.; Rodrigo, M.; Fernandez, F. J., A grey box model of glucose fermentation and  
483 syntrophic oxidation in microbial fuel cells. *Bioresource Technology* **2016**, 200, 396-404.
- 484 34. Lobato, J.; Cañizares, P.; Fernández, F. J.; Rodrigo, M. A., An evaluation of aerobic and  
485 anaerobic sludges as start-up material for microbial fuel cell systems. *New Biotechnology* **2012**, 29,  
486 (3), 415-420.

487